

Mutation of *ARHGEF18* causes adult-onset retinal degeneration and underscores a key role of apicobasal polarity proteins in the maintenance of human photoreceptors

Authors

Gavin Arno^{1,2}
Keren Carss^{3,4}
Sarah Hull^{1,2}
Ceniz Zihni¹
Anthony G Robson^{1,2}
Alessia Fiorentino¹
UK Inherited Retinal Disease Consortium
Alison J Hardcastle¹
Graham E Holder^{1,2}
Michael E Cheetham¹
Vincent Plagnol⁵
NIHR Bioresource Rare Diseases Consortium⁴
Anthony T Moore^{1,2,6}
F Lucy Raymond^{4,7}
Karl Matter¹
Maria S Balda¹
Andrew R Webster^{1,2}

1. UCL Institute of Ophthalmology, University College London, London EC1V 9EL, UK
2. Moorfields Eye Hospital, London EC1V 2PD, UK
3. Department of Haematology, University of Cambridge and, NHS Blood and Transplant, Cambridge CB2 0PT, UK
4. NIHR BioResource - Rare Diseases, Cambridge University Hospitals, Cambridge Biomedical Campus, Cambridge CB2 0QQ, UK.
5. University College London Genetics Institute, London WC1E 6BT, UK
6. Ophthalmology Department, UCSF School of Medicine, Koret Vision Centre, San Francisco CA 94133-0644, USA
7. Department of Medical Genetics, Cambridge Institute for Medical Research, University of Cambridge, Cambridge, CB2 0XY, UK

Abstract

Over 250 genes are implicated in inherited retinal dystrophy and encode proteins involved in a broad spectrum of pathways. Unsolved families following highly-parallel sequencing strategies suggest further genes remain to be identified. Whole exome and genome sequencing studies employed here in large cohorts of affected individuals revealed biallelic mutations in *ARHGEF18* in three such individuals. *ARHGEF18* encodes ARHGEF18 a guanine nucleotide exchange factor that activates RHOA, a small GTPase protein which is a key component of tight junctions and adherens junctions. This biological pathway is known to be important for retinal development and function, as mutation of *CRB1*, encoding another component, causes retinal dystrophy. The retinal structure in individuals with *ARHGEF18* mutations resembled that seen in those with *CRB1* mutations. Five mutations were

found on six alleles in the three individuals, specifically c.808A>G; p.Thr270Ala, c.1617+5G>A; p.Asp540Glyfs*63, c.1996C>T; p.Arg666*, c.2632G>T; p.Glu878* and c.2738_2761del; p.Arg913_Glu920del. Functional tests suggest that each disease genotype might retain some ARHGEF18 activity, such that the phenotype described here is not the consequence of nullizygosity. In particular, the p.Thr270Ala missense allele affects a highly conserved residue in the DBL homology domain, which is required for the interaction and activation of RHOA. Previously, knock-out of *Arhgef18* in the medaka fish has been shown to cause larval-lethality which is preceded by retinal defects that resemble those seen in zebra fish *Crumbs* complex knock-outs. The findings described here emphasise the peculiar sensitivity of the retina to perturbations of this pathway, which is highlighted as a target for potential therapeutic strategies.

Text

Inherited retinal dystrophy (IRD) encompasses a clinically and genetically heterogeneous group of disorders characterised by retinal dysfunction or degeneration. Variants in over 250 genes encoding proteins essential to a wide range of biological pathways including mRNA splicing, posttranslational protein modification, ciliogenesis, cilia protein transport, retinoid recycling in the visual cycle, phototransduction and retinal development, have been found causative of IRD (RetNet).

This present report describes mutation of *ARHGEF18* (MIM: 616432) as a likely cause of human IRD. The gene encodes ARHGEF18 (also known as p114RhoGEF)¹ the Rho/Rac guanine nucleotide exchange factor 18. It has been shown to be involved in the determination of apicobasal (AB) polarity in epithelia and cell-cell junction formation through its action on the small GTPase RHOA². The gene is widely expressed, with ESTs identified in many human tissues including the neurosensory retina (NCBI-UniGene).

The study protocol adhered to the tenets of the Declaration of Helsinki and received approval from the local ethics committee. Written, informed consent was obtained from all participants prior to their inclusion in this study. To gain further insight into the genetic pathology of inherited retinal dystrophy, whole exome sequencing (WES) has been performed on 230 individuals and whole genome sequencing (WGS) on a further 599 probands, ascertained from the inherited retinal disease clinics at Moorfields Eye Hospital (MEH), London. The latter cohort forms part of the NIHR-Bioresource Rare Disease consortium in the UK³.

Biallelic mutations in *ARHGEF18* were identified in 3 individuals (Table S1), presenting as simplex cases, each with a retinal dystrophy sharing features with that seen in retinal disease caused by *CRB1* (MIM: 604210)⁴. For this reason, in all three individuals, Sanger sequencing of the *CRB1* gene had been performed but did not identify any potential disease associated variants. WGS was performed on individuals 1 and 2; the remaining individual (individual 3) underwent WES as previously described⁵. In the first instance, resulting coding variant calls were filtered using a gene list of 236 genes

previously implicated in retinal dystrophy⁶. No convincing causal variants were identified in these affected individuals (Table S2).

Following WGS, individual 1 (GC18203), a 37 year old female with simplex retinitis pigmentosa (RP, MIM: 268000), the 2nd of 2 siblings born to unrelated parents with no family history of eye disease, had 20,863 coding (± 8 bp splice region) variants passing standard quality filters. Of these, 360 had a minor allele frequency (MAF) ≤ 0.01 in the publicly available dataset (Exome Aggregation Consortium database, ExAC). Assuming autosomal recessive inheritance, 5 genes contained ≥ 2 variants (Table S3). Variants were further manually interrogated for variant call quality, MAF in publicly available datasets and our own in-house exome sequencing dataset (UCL exome project of over 5000 individuals), predicted protein impact and biological plausibility (including protein function, expression profile and pathway analysis). Of these, two variants were identified in *ARHGEF18*. The variants, a missense and nonsense: GRCh37 (hg19) chr19:g.7509101A>G NM_001130955: c.808A>G, p.Thr270Ala ; chr19:g.7527145C>T NM_001130955: c.1996C>T, p.Arg666* were absent from ExAC. The missense variant (p.Thr270Ala) was predicted to be damaging by in silico prediction algorithms ("Sorting the intolerant from tolerant" [SIFT], Polymorphism Phenotyping v2 [PolyPhen-2])^{7,8} and affects a highly conserved amino acid residue in the DBL homology (DH) domain (Figure 1).

Identical analysis was performed on the 21,042 coding variants identified by WGS in individual 2 (GC3626), a 51 year old male simplex RP affected individual, the 2nd of 2 siblings born to unrelated parents with no family history of eye disease. Seventeen genes with ≥ 2 variants (MAF ≤ 0.01) were identified (Table S4), among which were two variants comprising a nonsense and in-frame deletion in *ARHGEF18*, chr19:g.7532286G>T NM_001130955: c.2632G>T, p.Glu878* ; chr19:g.7532392_7532415del NM_001130955:c.2738_2761del, p.Arg913_Glu920del. The two variants occur within 130bp in exon 16 of *ARHGEF18*. Interrogation of the 150bp paired end reads in this region using the Integrative Genomics Viewer (IGV)^{9,10} allowed phasing of the variants on 7 reads suggesting they were in *trans* (Figure 1c). Familial DNA samples were unavailable for segregation analysis. The in-frame deletion of 8 amino acid residues removes part of a highly conserved region of the protein (RLEQERAE) (Figure 1d).

Individual 3 (GC17880), an affected individual with simplex RP, the 2nd of 3 siblings born to 1st cousin parents with no family history of eye disease underwent WES revealing 21,404 coding variants. Of these, 383 were rare (MAF ≤ 0.01 in the publicly available NHLBI GO Exome Sequencing Project dataset [EVS]). Assuming recessive inheritance due to autozygosity, 7 genes had homozygous variants affecting the canonical transcript (Table S5), 6 of which were located within homozygous regions ≥ 5 Mb identified by prior SNP array autozygosity mapping data (SNP6, Affymetrix). Of these variants, a splice region substitution (chr19:g.7521294G>A NM_001130955: c.1617+5G>A) in *ARHGEF18* was the most compelling candidate. This variant is predicted to weaken the canonical splice donor site and lead to out of frame skipping of *ARHGEF18* exon 8.

The variants in each individual were confirmed to be biallelic by familial segregation analysis in all available relatives (Figure 1a); no unaffected family member available for screening carried two disease alleles. Subsequent direct Sanger sequencing of all coding exons of *ARHGEF18* in 10 individuals with a similar phenotype and no detectable mutation in *CRB1*⁴ revealed no further mutations in *ARHGEF18*. In a cohort of 5695 individuals who underwent WES (UCL-exome cohort), no rare (MAF≤0.01) loss of function (LOF) variants were identified, 4 individuals with unrelated phenotypes had predicted biallelic rare missense variants (Table S6).

The affected individuals reported here all presented in their 3rd – 4th decades with central visual disturbance, visual field defects and mild nyctalopia (Table S7). At last review at ages 37, 51 and 38 years for individuals 1, 2 and 3 respectively, visual acuity ranged from 0.18 log MAR (Snellen 20/30) to 1.8 log MAR (Snellen 20/1250) being worst in the oldest individual. Fundus examination revealed optic disc pallor, attenuated retinal vessels and irregular mid-peripheral intra-retinal pigment migration. Fundus autofluorescence (FAF) imaging revealed widespread, irregular, peripheral hypo-autofluorescence (Figure 2). Optical coherence tomography (OCT) demonstrated intra-retinal cysts in all affected individuals. Such imaging produces an in vivo cross-section of the retina. A useful landmark to gauge the degree of retinal degeneration is a contiguous line, parallel with the inner retinal surface, which is thought to be formed by reflection from mitochondria in photoreceptor inner segments, the so-called inner-segment ellipsoid line (ISe)¹¹. Individuals 1 and 3 had a preserved ISe throughout the macula; for Individual 2 the ISe was retained only in the foveal region. The irregularity of the autofluorescence is distinct from that occurring in primary rod photoreceptor disease and instead resembles that seen in *CRB1*-retinopathy. Moreover, peripheral nummular pigment was similar to *CRB1*-retinopathy. In most degenerative dystrophies the retina is thinner than normal, and in these individuals retinal thickness instead resembled that seen in *CRB1*-retinopathy. Full-field electroretinography (ERG), performed in all individuals at a similar age (29-30 years)¹², demonstrated severe generalized retinal dysfunction affecting rod more than cone photoreceptors (Figure S1). The pattern ERG¹³ was subnormal in individuals 1 and 3, indicating relatively mild macular involvement, but was undetectable in individual 2 consistent with severe macular involvement. There was no clinical evidence of other systemic, neurological or other epithelial disease in any of the individuals.

Cell-cell junctions, (Tight junctions [TJ] and adherens junctions [AJ]) are important in the establishment of apicobasal (AB) polarity. During vertebrate eye morphogenesis, AB polarity of epithelial cells forming the optic vesicle is established and maintained by the migration and accumulation of specific polarity proteins and lipid complexes and the regulation of actomyosin network in distinct apical and basal membrane domains and the formation of TJ and AJ^{14,15}. Interkinetic nuclear migration (IKNM) along the AB polarity axis results in specific positioning of nuclei in the single-cell neuroepithelium and a pseudostratified appearance, and in turn contributes to the cell fate determination during differentiation into the 3 nuclear layers of the retina¹⁶.

Three major classes of protein complexes have been implicated in the establishment and maintenance of AB polarity: the Crumbs, Par and Scribble complexes that serve as either apical or basolateral determinants. Rho small GTPase family members RHOA, RAC1 and CDC42 are central to the regulation of cell migration, contact adhesion and the regulation of these apical and basolateral determinants¹⁵. The genes encoding these GTPase family members have not been implicated in retinal disease^{15,17}. The activation status of Rho GTPases is determined by the guanine nucleotide bound to them (GTP-active, GDP-inactive), which is, in turn, regulated by guanine nucleotide exchange factors (GEF) and GTPase activating proteins (GAP).

Regulation of RHOA activation through ARHGEF18 is important for tissue morphogenesis and migration, and in the assembly and maintenance of cell-cell junctions, TJ and AJ^{14,15}. Cell junctions form intracellular connections essential for control of cell proliferation and morphology, and maintenance of tissue integrity. In epithelia, TJs are formed at the apical/lateral border and control the movement of molecules along the paracellular space¹⁸. Molecular mechanisms regulating RHOA activation are crucial components of the pathways that guide TJ assembly and function. ARHGEF18 drives RHOA activation at TJs and thereby regulates actomyosin activity and TJ assembly, epithelial morphology and dynamics^{2,19,20}.

Cell-cell junctions and AB polarity are essential in the function and maintenance of retinal architecture^{21,22}. In particular, the outer limiting membrane (OLM) is formed of AJs between Müller glia cells and photoreceptors and the inner/outer segments of photoreceptors are formed from the apical membrane of developing photoreceptors.

All of the individuals harbored genotypes of *ARHGEF18* that might conceivably produce some protein function, rather than being definite biallelic nulls. Individuals 1 and 2 had a nonsense mutation in *trans* with a missense or inframe deletion respectively. Reverse transcription-PCR (RT-PCR) and direct sequencing analysis of the *ARHGEF18* transcript from lymphocytes of individual 3 (c.1617+5G>A) using PCR primers spanning exon 6-9 identified differently spliced transcripts (Figure S2). Direct sequencing of the PCR-generated products identified a short transcript lacking exon 8 and a weaker band corresponding to the wild type (WT) transcript (including exon 8). Hence, a low proportion of WT transcript and full length WT protein is likely to be produced despite this splice-site alteration. Guanine to adenine transitions at position +5 in splice donor sites are recognised pathogenic mutations but have been reported previously to produce some normal mRNA product, for example in the context of cystic fibrosis²³. The downstream consequence of exon 8 skipping would be a termination codon following 62 out of frame codons (p.Asp540Glyfs*63) and a transcript that is likely to undergo nonsense mediated decay (NMD). The inframe deletion in individual 2, is predicted to abolish several putative exonic splice enhancer (ESE) motifs²⁴. However, RT-PCR and direct sequencing of the *ARHGEF18* transcript from lymphocytes of

individual 2 using PCR primers spanning exon 13-17 identified no alteration in splicing (Figure S2) as a consequence of the deletion.

In order to determine the functional consequence and potential pathogenicity of the missense and inframe deletion variants, HEK293T cells were transfected with expression vectors encoding wild-type (WT) *ARHGEF18* (NM_001130955)² or with the p.Thr270Ala substitution or the p.Arg913_Glu920del deletion generated using the Q5 site-directed mutagenesis kit (New England Biolabs, Hitchin, UK) according to manufacturers instructions and propagated, purified and sequenced using standard procedures. A previously characterized catalytically inactive mutant was included as a control (p.Tyr418Ala, previously referred to as p.Tyr260Ala)². RHOA activation is essential for ARHGEF18 to stimulate TJ assembly. This was tested by measuring RHOA-GTP levels in transfected HEK293T cells using a biochemical 96-well assay that measures binding of RHOA-GTP to the Rho binding domain of Rhotekin (G-LISA, Cytoskeleton, Inc.;²). Ectopic expression of the WT protein led to a more than 5-fold stimulation of RHOA-GTP levels (Figure 3A). The p.Thr270Ala mutant retained some activity compared to the catalytically inactive p.Tyr418Ala construct as it led to a 3-fold increase in RHOA-GTP levels, but was less than 50% of the WT level (Figure 3A). The deletion mutant (p.Arg913_Glu920del) had a similar increase in RHOA-GTP level to the WT protein (Figure 3A).

The transcriptional activity of serum response factor (SRF) was measured in transfected cells using a double luciferase reporter assay²⁵ to monitor signalling output of the mutant ARHGEF18 constructs. Similar to the RHOA activation assay, the WT construct led to a strong stimulation of SRF-driven luciferase expression while the missense mutant (p.Thr270Ala) led to a 3-fold reduction in the level of luciferase expression but, as in the RHOA-GTP assay, showed significant activity also if compared to the inactive p.Tyr418Ala mutant; the deletion mutant (p.Arg913_Glu920del) level was unaltered (Figure 3B). Thus, the p.Thr270Ala mutant led to reduced but not abolished RHOA activation and signalling, and the p.Arg913_Glu920del mutant did not affect RHOA activation.

As ARHGEF18 stimulates cortical actomyosin activation leading to TJ assembly and cell rounding in epithelial cells, human corneal epithelial cells (HCE) were transfected with the WT or mutant expression vectors, including the p.Tyr418Ala catalytically inactive control. Transfection of WT but not the p.Tyr418Ala control led to rounded morphology of the normally flat cells, increased cortical phospho-myosin (pp-MLC) and F-actin staining (Figure 3C). Similar to the GEF inactive mutant (p.Tyr418Ala), the p.Thr270Ala mutant was not recruited to the cell cortex and failed to induce the cortical actomyosin cytoskeleton enrichment (Figure 3C), supporting the conclusion that its activity was strongly reduced. The deletion mutant (p.Arg913_Glu920del) induced some cortical actomyosin reorganization, but appeared to do so less efficiently than WT. In addition, its distribution was more patchy and irregular than WT. Both mutations thus affect the normal subcellular localization of ARHGEF18. Only the WT protein induced a strong stimulation of recruitment of junctional proteins when overexpressed (Figure 3D). The two point

mutations (p.Thr270Ala, p.Tyr418Ala) failed to induce a response, and the deletion mutation led to cell rounding but only a weak increase in junctional recruitment of TJ markers alpha-catenin and Catenin delta-1, suggesting that the deletion inhibits the normal cellular activity of ARHGEF18 despite showing normal catalytic activity.

The missense mutation p.Thr270Ala resides within the DH domain of ARHGEF18, which is the catalytic domain required for guanine nucleotide exchange²⁶. Thr270 is located within the first alpha-helix of the highly conserved DH domain. This residue is conserved as a threonine or serine in virtually all DH domains throughout nature. In the *C.elegans* Rac GTPase activating protein, UNC-73, serine or threonine at this residue maintain the catalytic activity whereas mutation to alanine abolishes its activity^{26,27}. The hydroxyl group of the serine or threonine at this position in the DH domain is thought to mediate GTPase interaction, hence, substitution of Thr270 of ARHGEF18 may inhibit RHOA activation in this way.

The inframe deletion occurs in exon 16, downstream of the DH and PH module and does not directly interfere with the catalytic activity. The STK11 binding domain has been mapped to the C-terminal region of the murine ARHGEF18 protein encompassing these deleted amino acid residues and interaction of STK11 and ARHGEF18 is essential in AJ formation²⁸. Despite being catalytically active, the inframe deletion mutant appeared less potent for induction of cortical actomyosin organisation than the WT GEF, suggesting that the deletion may indeed affect interactions required for normal cellular ARHGEF18 function, possibly by removing residues required for interactions or for normal folding of the C-terminal domain.

The data indicate that all affected individuals retain some exchange factor activity or native protein. The strong reduction of ARHGEF18 function observed leads to the development of retinal dystrophy in these individuals but heterozygous carriers of LOF mutations are unaffected. The absence of a confirmed biallelic null in the cohort or indeed in the ExAC dataset suggests complete loss of ARHGEF18 function could be developmentally severe or lethal or may have a more syndromic phenotype. The hypothesis of an embryonic lethal phenotype is supported by the effect of null alleles in medaka fish²⁹.

Perturbation of the AB polarity of epithelial cells is recognised in tumorigenesis and cancer progression^{17,30,31} but, to date, only *CRB1* of the AB polarity complex encoding genes³² has been implicated in human Mendelian disease. Mutation of *CRB1* causes a wide spectrum of retinal disease including Leber congenital amaurosis (LCA), early onset retinal dystrophy (EORD), RP and more recently maculopathy and foveal retinoschisis^{33–36}. Age of onset and severity are variable, affected individuals often presenting with early onset severe loss of vision with characteristic sub-retinal white dots, deep nummular pigmentary lesions and a thickened, disorganised retina with an undetectable ERG in the most severe cases^{4,37}. It is of interest that the three individuals reported here resembled clinically those with *CRB1*-retinopathy although the age of onset was later⁴, and this suggests that

perturbation of this pathway produces a distinctive human retinal phenotype. The phenotypes of the murine *Crb1* knockout, *Crb1*^{-/-}, and naturally occurring *Rd8* truncating mutant are characterised by disruption of AJ between Müller cells and photoreceptors at the OLM, photoreceptor dysplasia and consequent focal areas of disorganised lamination and degeneration, although the remaining retina provides functional vision^{22,38,39}. The knock-in missense RP mutant *Crb*^{C249W} has a late onset degenerative phenotype and can partially rescue the phenotype in *Crb1*^{-/-} mice⁴⁰.

Mutation of the apical domain essential Crumbs complex proteins *epb41l5* (*moe*), *mpp5a* (*nok*) and *crb2a* (*ome*) in the zebrafish (*mosaic eyes*, *nagie oko* and *oko meduzy* respectively) all result in AB polarity defects leading to retinal dystrophy characterised by retinal developmental and lamination abnormalities⁴¹⁻⁴⁵. Similarly, the larval lethal medaka fish retinal differentiation mutant (*medeka* [*Japanese - large eyes*]) exhibits disorganisation of retinal lamination during embryonic development consequent on a LOF mutation resulting in absence of the ArhGEF18 protein product²⁹. The phenotype is consequent upon abrogation of ArhGEF18 activity in the developing embryo resulting in disruption of RHOA activation and perturbation of AB polarity characterised by mislocalisation of TJ, disorganisation of the actin cytoskeleton and cell proliferation morphology alterations.

The disease mechanism of human *ARHGEF18*-retinopathy is not yet fully understood and may include developmental and/or degenerative mechanisms. Disruption of ARHGEF18 function in retinal development seems unlikely, as a severe early onset retinal dystrophy would be a more probable consequence and our three individuals all experienced normal visual function in early life. A more plausible hypothesis is that photoreceptors are peculiarly sensitive to the failure of AJ maintenance than other cells causing onset of retinal degeneration in adulthood. Similar clinical features and variable age of onset seen in *CRB1*-retinopathy strengthens the assertion that maintenance of this complex is required for continued photoreceptor viability in humans. The phenotypic similarity of ArhGEF18 and crumbs complex protein knockouts in lower vertebrates reflects the similarity of these in humans. Taken together these observations suggest other proteins essential in AB polarity maintenance should be regarded as candidate genes in retinal dystrophies. Furthermore, the pathway provides a target for therapeutic intervention with the potential to ameliorate visual impairment due to this type of retinal dystrophy.

Consortia

UKIRDC (UK Inherited Retinal Dystrophy Consortium) members include Graeme Black, Georgina Hall, Stuart Ingram, Rachel Gillespie, Forbes Manson, Panagiotis Sergouniotis, Chris Inglehearn, Carmel Toomes, Manir Ali, Martin McKibbin, James Poulter, Kamron Khan, Emma Lord, Andrea Nemeth, Susan Downes, Stephanie Halford, Jing Yu, Stefano Lise, Gavin Arno, Alessia Fiorentino, Nikos Ponitkos, Vincent Plagnol, Michel Michaelides, Alison J. Hardcastle, Michael E. Cheetham, Andrew R. Webster, and Veronica van Heyningen.

Acknowledgements

This project was supported by The National Institute for Health Research (NIHR) and Biomedical Research Centre (BRC) at Moorfields Eye Hospital and the UCL Institute of Ophthalmology, RP Fighting Blindness, Fight For Sight UK, Moorfields Eye Hospital Special Trustees and Foundation Fighting Blindness - USA. KC was supported by grant funding from the NIHR Bioresource Rare Disease. The UKIRDC was funded by RP Fighting Blindness and Fight for Sight UK. MEC was supported by The Wellcome Trust, FLR was supported by Cambridge Biomedical Research Centre. The authors report no conflict of interest.

Web resources

Retnet: <https://sph.uth.edu/retnet/>

OMIM: <http://www.omim.org>

NCBI-UniGene: <https://www.ncbi.nlm.nih.gov/unigene>

ExAC: <http://exac.broadinstitute.org/>

EVS: <http://evs.gs.washington.edu/EVS/>

Clustal Omega: <http://www.ebi.ac.uk/Tools/msa/clustalo/>

Supplemental data

Supplemental data includes 7 tables and 2 figures.

References

1. Niu, J., Profirovic, J., Pan, H., Vaiskunaite, R., and Voyno-Yasenetskaya, T. (2003). G Protein betagamma subunits stimulate p114RhoGEF, a guanine nucleotide exchange factor for RhoA and Rac1: regulation of cell shape and reactive oxygen species production. *Circ. Res.* 93, 848–856.
2. Terry, S.J., Zihni, C., Elbediwy, A., Vitiello, E., Leefa Chong San, I. V., Balda, M.S., and Matter, K. (2011). Spatially restricted activation of RhoA signalling at epithelial junctions by p114RhoGEF drives junction formation and morphogenesis. *Nat. Cell Biol.* 13, 159–166.
3. Arno, G., Hull, S., Carss, K., Dev-Borman, A., Chakarova, C., Bujakowska, K., van den Born, I., Robson, A.G., Holder, G.E., Michaelides, M., et al. (2016). Reevaluation of the Retinal Dystrophy Due to Recessive Alleles of RGR With the Discovery of a Cis-Acting Mutation in CDHR1. *Invest. Ophthalmol. Vis. Sci.* 57, 4806–4813.
4. Henderson, R.H., Mackay, D.S., Li, Z., Moradi, P., Sergouniotis, P., Russell-Eggitt, I., Thompson, D.A., Robson, A.G., Holder, G.E., Webster,

A.R., et al. (2011). Phenotypic variability in patients with retinal dystrophies due to mutations in CRB1. *Br. J. Ophthalmol.* 95, 811–817.

5. Arno, G., Hull, S., Robson, A.G., Holder, G.E., Cheetham, M.E., Webster, A.R., Plagnol, V., and Moore, A.T. (2015). Lack of interphotoreceptor retinoid binding protein, caused by homozygous mutation of RBP3, is associated with high myopia and retinal dystrophy. *Invest. Ophthalmol. Vis. Sci.* 56, 2358–2365.

6. Carss, K.J., Arno, G., Erwood, M., Stephens, J., Sanchis-Juan, A., Hull, S., Megy, K., Grozeva, D., Dewhurst, E., Malka, S., et al. (2017). Comprehensive rare variant analysis using whole genome sequencing to determine the molecular pathology of inherited retinal disease. *Am. J. Hum. Genet.* *in press*.

7. Kumar, P., Henikoff, S., and Ng, P.C. (2009). Predicting the effects of coding non-synonymous variants on protein function using the SIFT algorithm. *Nat. Protoc.* 4, 1073–1081.

8. Adzhubei, I.A., Schmidt, S., Peshkin, L., Ramensky, V.E., Gerasimova, A., Bork, P., Kondrashov, A.S., and Sunyaev, S.R. (2010). A method and server for predicting damaging missense mutations. *Nat. Methods* 7, 248–249.

9. Robinson, J.T., Thorvaldsdóttir, H., Winckler, W., Guttman, M., Lander, E.S., Getz, G., and Mesirov, J.P. (2011). Integrative genomics viewer. *Nat. Biotechnol.* 29, 24–26.

10. Thorvaldsdóttir, H., Robinson, J.T., and Mesirov, J.P. (2013). Integrative Genomics Viewer (IGV): high-performance genomics data visualization and exploration. *Brief. Bioinform.* 14, 178–192.

11. Spaide, R.F., and Curcio, C.A. (2011). Anatomical correlates to the bands seen in the outer retina by optical coherence tomography: literature review and model. *Retina* 31, 1609–1619.

12. McCulloch, D.L., Marmor, M.F., Brigell, M.G., Hamilton, R., Holder, G.E., Tzekov, R., and Bach, M. (2015). ISCEV Standard for full-field clinical electroretinography (2015 update). *Doc. Ophthalmol.* 130, 1–12.

13. Bach, M., Brigell, M.G., Hawlina, M., Holder, G.E., Johnson, M.A., McCulloch, D.L., Meigen, T., and Viswanathan, S. (2013). ISCEV standard for clinical pattern electroretinography (PERG): 2012 update. *Doc Ophthalmol* 126, 1–7.

14. Loosli, F. ArhGEF18 regulated Rho signaling in vertebrate retina development. *Small GTPases* 4, 242–246.

15. Mack, N.A., and Georgiou, M. (2014). The interdependence of the Rho GTPases and apicobasal cell polarity. *Small GTPases.* 5, 10.

16. Norden, C., Young, S., Link, B.A., and Harris, W.A. (2009). Actomyosin is the main driver of interkinetic nuclear migration in the retina. *Cell* 138, 1195–1208.
17. Royer, C., and Lu, X. (2011). Epithelial cell polarity: a major gatekeeper against cancer? *Cell Death Differ.* 18, 1470–1477.
18. Zihni, C., Mills, C., Matter, K., and Balda, M.S. (2016). Tight junctions: from simple barriers to multifunctional molecular gates. *Nat. Rev. Mol. Cell Biol.* 17, 564–80.
19. Terry, S.J., Elbediwy, A., Zihni, C., Harris, A.R., Bailly, M., Charras, G.T., Balda, M.S., and Matter, K. (2012). Stimulation of cortical myosin phosphorylation by p114RhoGEF drives cell migration and tumor cell invasion. *PLoS One* 7, e50188.
20. Blomquist, A., Schwörer, G., Schablowski, H., Psoma, A., Lehnen, M., Jakobs, K.H., and Rümenapp, U. (2000). Identification and characterization of a novel Rho-specific guanine nucleotide exchange factor. *Biochem. J.* 352 Pt 2, 319–325.
21. Van de Pavert, S.A., Sanz, A.S., Aartsen, W.M., Vos, R.M., Versteeg, I., Beck, S.C., Klooster, J., Seeliger, M.W., and Wijnholds, J. (2007). Crb1 is a determinant of retinal apical Müller glia cell features. *Glia* 55, 1486–1497.
22. Mehalow, A.K., Kameya, S., Smith, R.S., Hawes, N.L., Denegre, J.M., Young, J.A., Bechtold, L., Haider, N.B., Tepass, U., Heckenlively, J.R., et al. (2003). CRB1 is essential for external limiting membrane integrity and photoreceptor morphogenesis in the mammalian retina. *Hum. Mol. Genet.* 12, 2179–2189.
23. Duguépéroux, I., and De Braekeleer, M. (2005). The CFTR 3849+10kbC->T and 2789+5G->A alleles are associated with a mild CF phenotype. *Eur. Respir. J.* 25, 468–473.
24. Desmet, F.-O., Hamroun, D., Lalande, M., Collod-Bérout, G., Claustres, M., and Bérout, C. (2009). Human Splicing Finder: an online bioinformatics tool to predict splicing signals. *Nucleic Acids Res.* 37, e67.
25. Tsapara, A., Luthert, P., Greenwood, J., Hill, C.S., Matter, K., and Balda, M.S. (2010). The RhoA activator GEF-H1/Lfc is a transforming growth factor-beta target gene and effector that regulates alpha-smooth muscle actin expression and cell migration. *Mol. Biol. Cell* 21, 860–870.
26. Aghazadeh, B., Zhu, K., Kubiseski, T.J., Liu, G.A., Pawson, T., Zheng, Y., and Rosen, M.K. (1998). Structure and mutagenesis of the Dbl homology domain. *Nat. Struct. Biol.* 5, 1098–1107.
27. Steven, R., Kubiseski, T.J., Zheng, H., Kulkarni, S., Mancillas, J., Ruiz Morales, A., Hogue, C.W., Pawson, T., and Culotti, J. (1998). UNC-73

activates the Rac GTPase and is required for cell and growth cone migrations in *C. elegans*. *Cell* 92, 785–795.

28. Xu, X., Jin, D., Durgan, J., and Hall, A. (2013). LKB1 controls human bronchial epithelial morphogenesis through p114RhoGEF-dependent RhoA activation. *Mol. Cell. Biol.* 33, 2671–2682.

29. Herder, C., Swiercz, J.M., Müller, C., Peravali, R., Quiring, R., Offermanns, S., Wittbrodt, J., and Loosli, F. (2013). ArhGEF18 regulates RhoA-Rock2 signaling to maintain neuro-epithelial apico-basal polarity and proliferation. *Development* 140, 2787–2797.

30. Etienne-Manneville, S. (2008). Polarity proteins in migration and invasion. *Oncogene* 27, 6970–6980.

31. Martin-Belmonte, F., and Perez-Moreno, M. (2012). Epithelial cell polarity, stem cells and cancer. *Nat. Rev. Cancer* 12, 23–38.

32. Assémat, E., Bazellières, E., Pallesi-Pocachard, E., Le Bivic, A., and Massey-Harroche, D. (2008). Polarity complex proteins. *Biochim. Biophys. Acta - Biomembr.* 1778, 614–630.

33. Den Hollander, A.I., ten Brink, J.B., de Kok, Y.J., van Soest, S., van den Born, L.I., van Driel, M.A., van de Pol, D.J., Payne, A.M., Bhattacharya, S.S., Kellner, U., et al. (1999). Mutations in a human homologue of *Drosophila* crumbs cause retinitis pigmentosa (RP12). *Nat. Genet.* 23, 217–221.

34. Lotery, A.J., Jacobson, S.G., Fishman, G.A., Weleber, R.G., Fulton, A.B., Namperumalsamy, P., Héon, E., Levin, A. V, Grover, S., Rosenow, J.R., et al. (2001). Mutations in the CRB1 gene cause Leber congenital amaurosis. *Arch. Ophthalmol. (Chicago, Ill. 1960)* 119, 415–420.

35. Tsang, S.H., Burke, T., Oll, M., Yzer, S., Lee, W., Xie, Y.A., and Allikmets, R. (2014). Whole exome sequencing identifies CRB1 defect in an unusual maculopathy phenotype. *Ophthalmology* 121, 1773–1782.

36. Vincent, A., Ng, J., Gerth-Kahlert, C., Tavares, E., Maynes, J.T., Wright, T., Tiwari, A., Tumber, A., Li, S., Hanson, J.V.M., et al. (2016). Biallelic Mutations in CRB1 Underlie Autosomal Recessive Familial Foveal Retinoschisis. *Invest. Ophthalmol. Vis. Sci.* 57, 2637–2646.

37. Jacobson, S.G., Cideciyan, A. V, Aleman, T.S., Pianta, M.J., Sumaroka, A., Schwartz, S.B., Smilko, E.E., Milam, A.H., Sheffield, V.C., and Stone, E.M. (2003). Crumbs homolog 1 (CRB1) mutations result in a thick human retina with abnormal lamination. *Hum. Mol. Genet.* 12, 1073–1078.

38. Aleman, T.S., Cideciyan, A. V, Aguirre, G.K., Huang, W.C., Mullins, C.L., Roman, A.J., Sumaroka, A., Olivares, M.B., Tsai, F.F., Schwartz, S.B., et al. (2011). Human CRB1-associated retinal degeneration: comparison with the rd8 Crb1-mutant mouse model. *Invest. Ophthalmol. Vis. Sci.* 52, 6898–6910.

39. Van de Pavert, S.A., Kantardzhieva, A., Malysheva, A., Meuleman, J., Versteeg, I., Levelt, C., Klooster, J., Geiger, S., Seeliger, M.W., Rashbass, P., et al. (2004). Crumbs homologue 1 is required for maintenance of photoreceptor cell polarization and adhesion during light exposure. *J. Cell Sci.* **117**, 4169–4177.
40. Van de Pavert, S.A., Meuleman, J., Malysheva, A., Aartsen, W.M., Versteeg, I., Tonagel, F., Kamphuis, W., McCabe, C.J., Seeliger, M.W., and Wijnholds, J. (2007). A single amino acid substitution (Cys249Trp) in Crb1 causes retinal degeneration and deregulates expression of pituitary tumor transforming gene Pttg1. *J. Neurosci.* **27**, 564–573.
41. Wei, X., and Malicki, J. (2002). *nagie oko*, encoding a MAGUK-family protein, is essential for cellular patterning of the retina. *Nat. Genet.* **31**, 150–157.
42. Jensen, A.M., Walker, C., and Westerfield, M. (2001). *mosaic eyes*: a zebrafish gene required in pigmented epithelium for apical localization of retinal cell division and lamination. *Development* **128**, 95–105.
43. Hsu, Y.-C., Willoughby, J.J., Christensen, A.K., and Jensen, A.M. (2006). *Mosaic Eyes* is a novel component of the Crumbs complex and negatively regulates photoreceptor apical size. *Development* **133**, 4849–4859.
44. Omori, Y., and Malicki, J. (2006). *oko meduzy* and related crumbs genes are determinants of apical cell features in the vertebrate embryo. *Curr. Biol.* **16**, 945–957.
45. Malicki, J., and Driever, W. (1999). *oko meduzy* mutations affect neuronal patterning in the zebrafish retina and reveal cell-cell interactions of the retinal neuroepithelial sheet. *Development* **126**, 1235–1246.

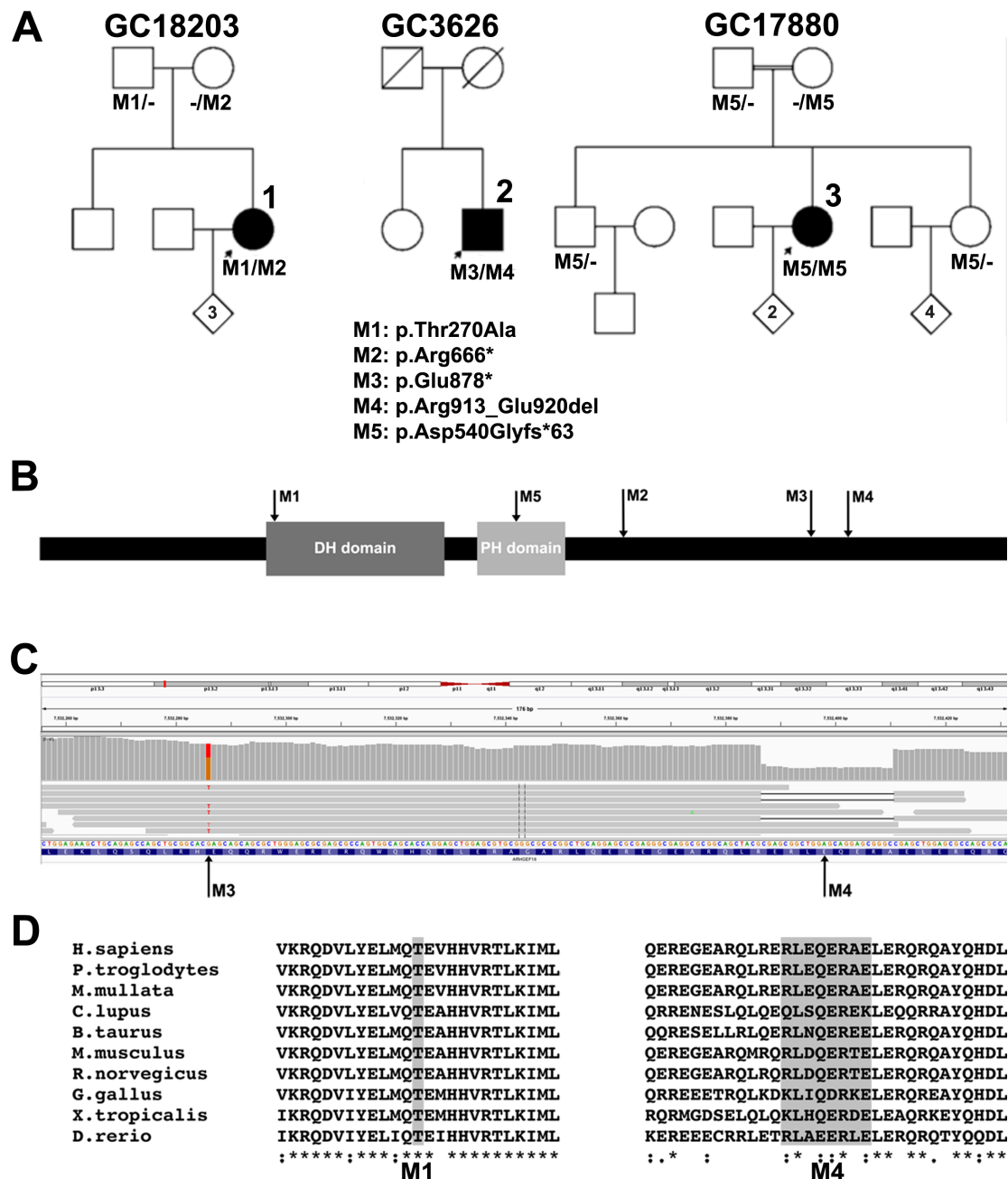


Figure 1: Variant analysis of *ARHGEF18* in individuals 1-3. **A.** Pedigrees and cosegregation of mutations M1-M5 in families 1-3. **B.** Schematic representation of mutation location in full length *ARHGEF18* protein including DBL homology (DH) and Plekstrin homology (PH) domains. **C.** IGV visualisation of 150bp paired end reads spanning mutations *ARHGEF18*, c.2632G>T and c.2738_2761del in individual 2, showing biallelic state. **D.** Clustal Omega alignment of amino acid residues affected by M1 (missense) and M4 (inframe deletion) mutations throughout vertebrate orthologues.

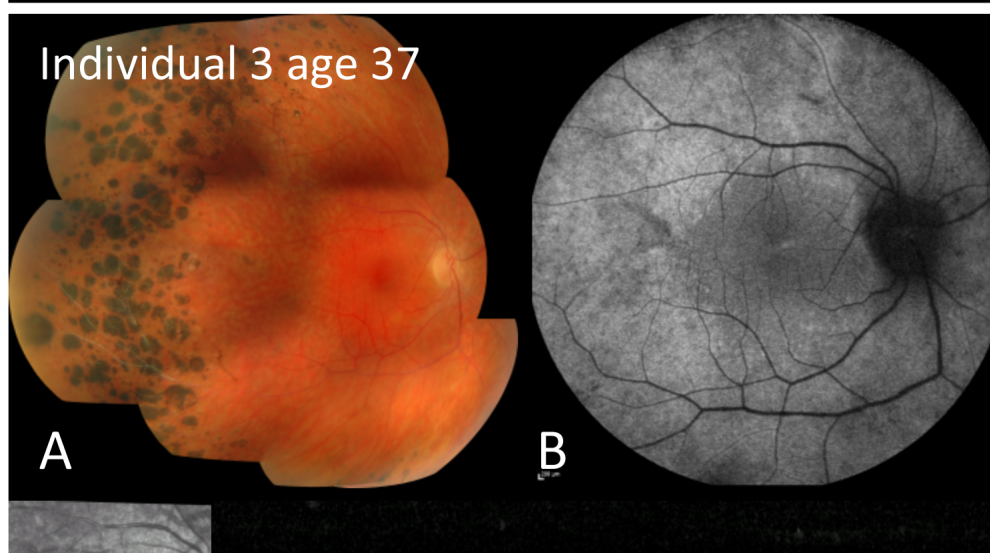
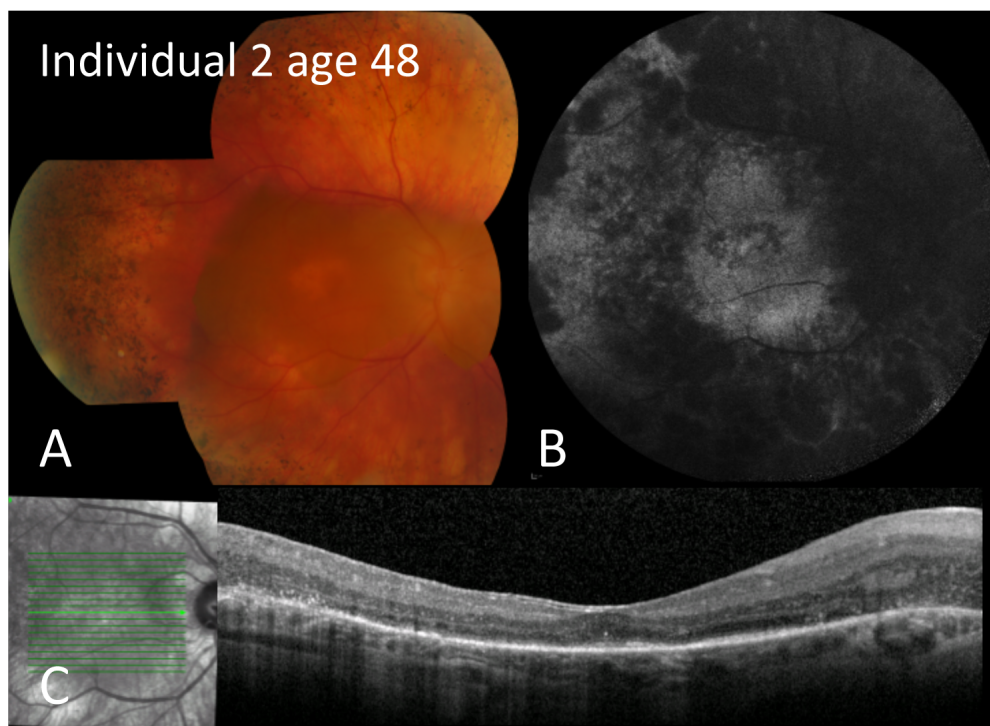
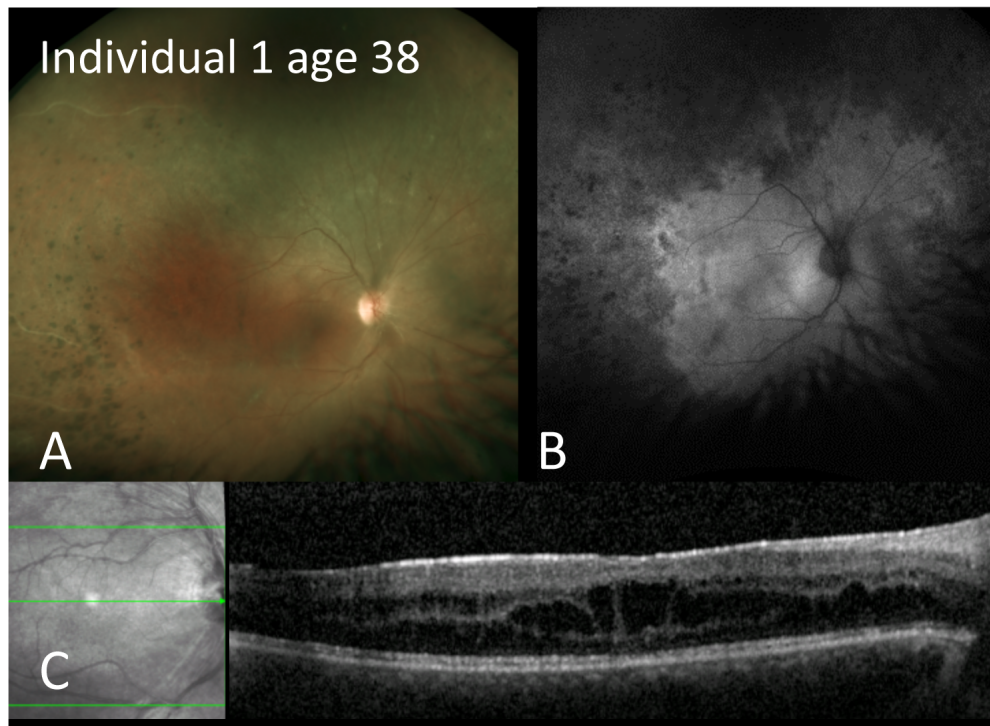
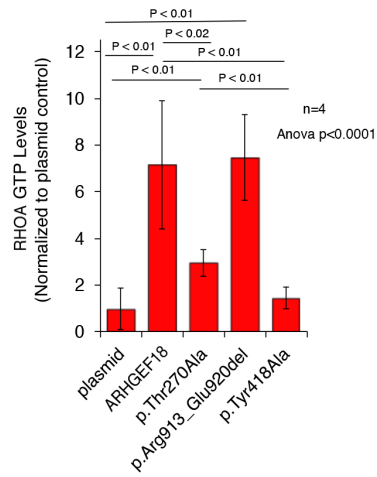
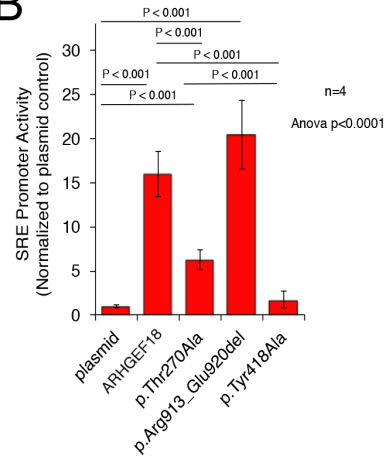


Figure 2: Retinal abnormalities in *ARHGEF18* related retinal dystrophy. **A.** Color fundus photographs, 55 degree fundus autofluorescence imaging, and optical coherence tomography (OCT). Individual 1, right eye at age 38 years : **A.** optic disc pallor, peripheral retinal pigment epithelium (RPE) atrophy and nummular pigmentation; **B.** peripheral patchy reduction of autofluorescence; **C.** reasonably preserved retinal layers on OCT with disruption of the inner segment ellipsoid band and intra-retinal cysts within the inner nuclear layer. Individual 2, right eye at 48 years: **D.** disc pallor and vessels attenuation with RPE atrophy within the macula and mid-periphery as well as peripheral nummular and dot lesions of hyperpigmentation; **E.** extensive loss of autofluorescence in periphery and in a central ring in macula; **F.** loss of outer retina and RPE throughout the macula with small foci of preserved photoreceptors centrally. Individual 3, right eye at 37 years: **G.** vascular attenuation and occlusion, peripheral RPE atrophy, white dots and nummular pigmentation; **H.** loss of autofluorescence in periphery; **I.** reasonably preserved retinal layers on OCT with disruption of the inner segment ellipsoid band and intra-retinal cysts within the inner nuclear layer.

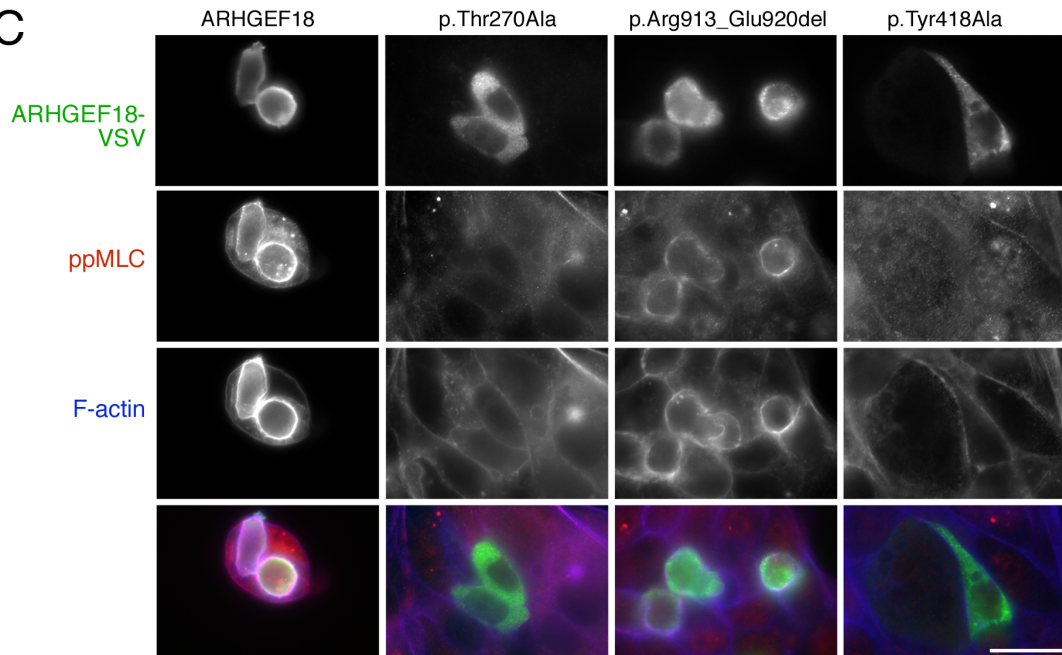
A



B



C



D

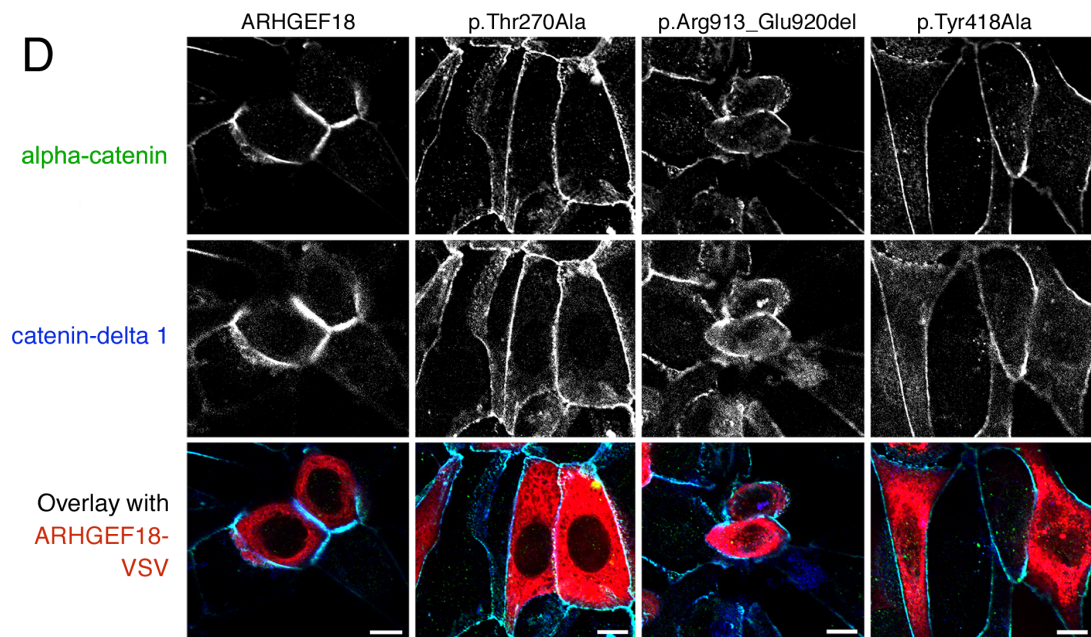


Figure 3: Signalling activity of ARHGEF18 variants. HEK293T or HCE cells were transfected with cDNAs encoding wild type or mutant VSV-tagged ARHGEF18. **A.** Lysates of transfected HEK293T cells were assayed for RHOA-GTP levels by G-LISA assay, which measures binding of active RHOA to the GTPase binding domain of Rhotekin. **B.** Serum response element (SRE) element activity was measured using a double luciferase assay with an SRE-containing promoter driving firefly luciferase expression and a CMV promoter expression of renilla luciferase. Firefly to renilla luciferase ratios were calculated and normalized to a plasmid control performed by co-transfecting an empty expression vector. The graphs show averages \pm 1 standard deviations, n=4, indicated are p-values from Anova and t-tests. **C.** Transfected HCE cells were fixed and stained with anti-VSV and anti-phosphorylated myosin regulatory light chain (ppMLC) antibodies along Ato-647-labelled phalloidin to visualize F-actin and imaged by epifluorescence. **D.** Cells transfected as in D were stained for the junctional markers alpha-catenin and Catenin delta-1 and imaged by confocal microscopy. Scale bars: C, 20 μ m; D, 10 μ m.

Supplemental data

Table S1: Summary of *ARHGEF18* mutations

	Individual	Genomic coordinates (GRCh37)	cDNA change (NM_001130955)	Protein consequence
M1	1	chr19:g.7509101A>G	c.808A>G	p.Thr270Ala
M2	1	chr19:g.7527145C>T	c.1996C>T	p.Arg666*
M3	2	chr19:g.7532286G>T	c.2632G>T	p.Glu878*
M4	2	chr19:g.7532392_ 7532415del	c.2738_2761del	p.Arg913_Glu920del
M5	3	chr19:g.7521294G>A	c.1617+5G>A	p.Asp540Glyfs*63
Control	N/A	N/A	c.1252_1253delTAinsGC	p.Tyr418Ala

(Control: GEF inactive mutant construct)

Table S2: Rare variants observed in genes associated with IRD in individuals 1-3

Individual	HUGO	Genotype	HGVSc	HGVSp	EXAC_AF	Disease inheritance	Exclusion criteria
1	GPR98	Heterozygous	ENST00000405460.2: c.2288A>G	ENSP00000384582.2: p.Asp763Gly	NA	Recessive	Heterozygous variant only/ does not fit phenotype
1	NPHP3	Heterozygous	ENST00000337331.5: c.1189C>T	ENSP00000338766.5: p.Arg397Cys	0.003303	Recessive	Heterozygous variant only/ does not fit phenotype
1	GUCA1B	Heterozygous	ENST00000230361.3: c.253G>A	ENSP00000230361.3: p.Val85Met	0.001359	Dominant	ExAC MAF too high for dominant disease allele
1	MYO7A	Heterozygous	ENST00000409709.3: c.3392A>G	ENSP00000386331.3: p.His1131Arg	0.000008411	Recessive	Heterozygous variant only/ does not fit phenotype
1	CDH23	Heterozygous	ENST00000398788.3: c.1591G>A	ENSP00000381768.3: p.Gly531Ser	0.0004793	Recessive	Heterozygous variant only/ does not fit phenotype
1	PROM1	Heterozygous	ENST00000510224.1: c.622delA	ENSP00000426809.1: p.Thr208LeufsTer23	0.00005793	Dominant/recessive	Biallelic LOF variants in PROM1 cause arRP - This individual is a carrier of a probable LOF allele in PROM1
1	RP1	Heterozygous	ENST00000220676.1: c.1118C>T	ENSP00000220676.1: p.Thr373Ile	0.013	Dominant/recessive	ExAC MAF too high for dominant disease allele
2	PEX1	Heterozygous	ENST00000248633.4: c.1276A>G	ENSP00000248633.4: p.Met426Val	0.000008237	Recessive	Heterozygous variant only/ does not fit phenotype
2	ABCC6	Heterozygous	ENST00000205557.7: c.2836C>A	ENSP00000205557.7: p.Leu946Ile	0.011	Recessive	Does not fit phenotype
2	ABCC6	Heterozygous	ENST00000205557.7: c.3507-3C>T		0.016	Recessive	Does not fit phenotype
2	MAK	Heterozygous	ENST00000313243.2: c.174T>G	ENSP00000313021.2: p.Asn58Lys	0.0002069	Recessive	Heterozygous variant only
2	HMX1	Heterozygous	ENST00000400677.3: c.233G>A	ENSP00000383516.3: p.Gly78Asp	NA	Recessive	Heterozygous variant only
2	AHI1	Heterozygous	ENST00000367800.4: c.2961+7_2961+21del TTATTTTATGCAGTTi nsGACTTTTTTAAAG TTTTAA		NA	Recessive	Heterozygous variant only
2	SLC24A1	Heterozygous	ENST00000261892.6: c.2813T>G	ENSP00000261892.6: p.Val938Gly	0.000008276	Recessive	Heterozygous variant only/ does not fit phenotype
2	IDH3B	Heterozygous	ENST00000380851.5: c.1133C>T	ENSP00000370232.5: p.Ala378Val	0.00003295	Recessive	Heterozygous variant only
2	ARL13B	Heterozygous	ENST00000394222.3: c.1186C>G	ENSP00000377769.3: p.Pro396Ala	0.006466	Recessive	Heterozygous variant only/ does not fit phenotype

2	IMPDH1	Heterozygous	ENST00000338791.6: c.1108G>A	ENSP00000345096.6: p.Ala370Thr	0.002224	Dominant	ExAC MAF too high for dominant disease allele
2	COL18A1	Heterozygous	ENST00000359759.4: c.1210G>A	ENSP00000352798.4: p.Ala404Thr	0.001865	Recessive	Heterozygous variant only/ does not fit phenotype
2	IMPG2	Heterozygous	ENST00000193391.7: c.3038C>T	ENSP00000193391.6: p.Pro1013Leu	0.003533	Recessive	Heterozygous variant only
2	BBS12	Heterozygous	ENST00000542236.1: c.1190C>T	ENSP00000438273.1: p.Ala397Val	0.00001647	Recessive	Heterozygous variant only/ does not fit phenotype
2	PDE6A	Heterozygous	ENST00000255266.5: c.718-4dupT		0.002018	Recessive	Heterozygous variant only
2	CDHR1	Heterozygous	ENST00000372117.3: c.1868A>G	ENSP00000361189.3: p.Asn623Ser	0.004093	Recessive	Heterozygous variant only
2	BBS2	Heterozygous	ENST00000245157.5: c.1231A>G	ENSP00000245157.5: p.Ile411Val	NA	Recessive	Heterozygous variant only/ does not fit phenotype
3	ABCA4	Heterozygous	ENST00000370225:ex on9:c.1140T>A	ENSP00000359245.3: p.Asn380Lys	0.0004942	Recessive	Heterozygous variant only/ does not fit phenotype
3	GNAT2	Heterozygous	ENST00000351050:ex on8:c.896C>T	ENSP00000251337.3: p.Ala299Val	0.00004122	Recessive	Heterozygous variant only/ does not fit phenotype
3	USH2A	Heterozygous	ENST00000307340:ex on15:c.3026C>G	ENSP00000305941.3: p.Ala1009Gly	0.000008347	Recessive	Heterozygous variant only
3	TRPM1	Heterozygous	ENST00000397795:ex on27:c.3841G>A	ENSP00000380897.2: p.Glu1281Lys	0.006526	Recessive	Heterozygous variant only/ does not fit phenotype

Table S3: Predicted biallelic rare variants observed in individual 1:

CHR	POSITION	REFERENCE	OBSERVED	Genotype	EXAC_AF	HUGO	CONSEQUENCE	HGVSc	HGVSp
1	33235594	C	T	HET	2.49E-05	KIAA1522	missense_variant	ENST00000401073.2:c.814C>T	ENSP00000383851.2:p.Arg272Trp
1	33237743	C	G	HET	5.79E-05	KIAA1522	missense_variant	ENST00000401073.2:c.2963C>G	ENSP00000383851.2:p.Ser988Cys
1	53793511	T	A	HOM	0.0009537	LRP8	missense_variant	ENST00000306052.6:c.74A>T	ENSP00000303634.6:p.Gln25Leu
2	189899700	T	A	HET	0.0004942	COL5A2	missense_variant	ENST00000374866.3:c.4295A>T	ENSP00000364000.3:p.Asp1432Val
2	189899755	C	T	HET	0.0009884	COL5A2	missense_variant	ENST00000374866.3:c.4240G>A	ENSP00000364000.3:p.Asp1414Asn
19	7509101	A	G	HET	NA	ARHGEF18	missense_variant	ENST00000359920.6:c.808A>G	ENSP00000352995.4:p.Thr270Ala
19	7527145	C	T	HET	NA	ARHGEF18	stop_gained	ENST00000359920.6:c.1996C>T	ENSP00000352995.4:p.Arg666Ter
22	46654636	G	C	HET	0.0008484	PKDREJ	missense_variant	ENST00000253255.5:c.4584C>G	ENSP00000253255.5:p.Ile1528Met
22	46658832	C	T	HET	NA	PKDREJ	missense_variant	ENST00000253255.5:c.388G>A	ENSP00000253255.5:p.Val130Met

Table S4: Predicted biallelic rare variants observed in individual 2:

CHR	POSITION	REFERENCE	OBSERVED	Genotype	EXAC_AF	HUGO	CONSEQUENCE	HGVSc	HGVSp
2	152376170	A	G	HET	0.0001159	NEB	splice_donor_variant	ENST00000397345.3:c.22590+2T>C	
2	152584331	T	TGCTGGCT GTGCCAGA	HET	NA	NEB	inframe_insertion	ENST00000397345.3:c.153_167dupTCTGGCACAGCCAGC	ENSP00000380505.3:p.Leu57_Ala61dup
3	65425560	TCTGCTGCT G	T	HOM	NA	MAGI1	inframe_deletion	ENST00000402939.2:c.1255_1263delCAGCAGCAG	ENSP00000385450.2:p.Gln419_Gln421del
4	187584530	G	A	HOM	0.004081	FAT1	missense_variant	ENST00000441802.2:c.3503C>T	ENSP00000406229.2:p.Ser1168Leu
5	77311370	C	T	HET	0.003805	AP3B1	missense_variant&splice_region_variant	ENST00000255194.6:c.2995G>A	ENSP00000255194.6:p.Val999Met
5	77461466	C	G	HET	0.0005687	AP3B1	missense_variant	ENST00000255194.6:c.1198G>C	ENSP00000255194.6:p.Ala400Pro
7	100674881	G	A	HET	0.0002586	MUC17	splice_acceptor_variant	ENST00000306151.4:c.185-1G>A	n/a
7	100685397	G	A	HET	0.0001071	MUC17	missense_variant	ENST00000306151.4:c.1070G>A	ENSP00000302716.4:p.Arg356His
8	21974516	C	T	HET	0.0006927	HR	missense_variant	ENST00000381418.4:c.3250G>A	ENSP00000370826.4:p.Ala1084Thr
8	21978273	G	A	HET	0.0004436	HR	missense_variant	ENST00000381418.4:c.2566C>T	ENSP00000370826.4:p.Arg856Trp
12	58016602	AGCTGCCCA GGATTCTG	A	HET	0.001812	SLC26A10	frameshift_variant	ENST00000320442.4:c.829_844delCCCAGGATTCTGGCTG	ENSP00000320217.4:p.Pro277ThrfsTer138
12	58016690	G	C	HET	0.001738	SLC26A10	missense_variant	ENST00000320442.4:c.912G>C	ENSP00000320217.4:p.Lys304Asn
12	58016890	T	G	HET	0.003328	SLC26A10	missense_variant	ENST00000320442.4:c.1023T>G	ENSP00000320217.4:p.Asn341Lys
14	45711988	C	A	HET	0.003706	MIS18BP1	missense_variant	ENST00000310806.4:c.634G>T	ENSP00000309790.4:p.Ala212Ser
14	45712000	G	C	HET	0.0007413	MIS18BP1	missense_variant	ENST00000310806.4:c.622C>G	ENSP00000309790.4:p.Gln208Glu
14	102900798	T	G	HET	0.0009748	TECPR2	missense_variant	ENST00000359520.7:c.1644T>G	ENSP00000352510.7:p.Asn548Lys
14	102916165	C	T	HET	0.00411	TECPR2	missense_variant	ENST00000359520.7:c.3275C>T	ENSP00000352510.7:p.Ser1092Leu
16	16255424	G	A	HET	0.016	ABCC6	splice_region_variant&intron_variant	ENST00000205557.7:c.3507-3C>T	n/a
16	16263662	G	T	HET	0.011	ABCC6	missense_variant	ENST00000205557.7:c.2836C>A	ENSP00000205557.7:p.Leu946Ile

16	23646857	A	G	HOM	0.014	PALB2	missense_variant	ENST00000261584.4:c.1010T>C	ENSP00000261584.4:p.Leu337Ser
16	31475712	C	A	HET	0.0002853	ARMC5	splice_region_variant&intron_variant	ENST00000268314.4:c.1371-3C>A	n/a
16	31477594	C	G	HET	0.001536	ARMC5	missense_variant	ENST00000268314.4:c.2192C>G	ENSP00000268314.4:p.Pro731Arg
16	88782205	G	C	HET	0.0009697	PIEZO1	missense_variant	ENST00000301015.9:c.7374C>G	ENSP00000301015.9:p.Phe2458Leu
16	88789499	G	A	HET	0.001903	PIEZO1	splice_region_variant&intron_variant	ENST00000301015.9:c.4495+4C>T	n/a
16	88798919	G	T	HET	0.0009696	PIEZO1	missense_variant	ENST00000301015.9:c.2815C>A	ENSP00000301015.9:p.Leu939Met
17	55183792	GGCTTGGATAGAAATGAGGAGA	G	HOM	NA	AKAP1	inframe_deletion	ENST00000337714.3:c.988_1008delAGCTTGGATAGAAATGAGGAG	ENSP00000337736.3:p.Ser330_Glu336del
19	7532286	G	T	HET	NA	ARHGEF18	stop_gained	ENST00000359920.6:c.2632G>T	ENSP00000352995.4:p.Glu878Ter
19	7532386	GCGAGCGGCTGGAGCAGGACGGGC	G	HET	NA	ARHGEF18	inframe_deletion	ENST00000359920.6:c.2738_2761delGGCTGGAGCAGGACGGGCCGAGC	ENSP00000352995.4:p.Arg913_Glu920del
19	8130867	G	T	HET	0.002926	FBN3	missense_variant	ENST00000600128.1:c.8366C>A	ENSP00000470498.1:p.Pro2789Gln
19	8138104	C	T	HET	0.003295	FBN3	missense_variant	ENST00000600128.1:c.7780G>A	ENSP00000470498.1:p.Val2594Ile
22	46760604	C	T	HET	0.0003229	CELSR1	missense_variant	ENST00000262738.3:c.8584G>A	ENSP00000262738.3:p.Gly2862Ser
22	46762275	G	A	HET	1.67E-05	CELSR1	splice_region_variant&intron_variant	ENST00000262738.3:c.8300+8C>T	n/a

Table S5: Predicted biallelic rare variants observed in individual 3:

CHR	POSITION	REFERENCE	OBSERVED	Genotype	EVS MAF	HUGO	Exonic Function	AAChange	
1	158908291	C	G	HET	NA	PYHIN1	nonsynonymous SNV	ENST00000368140:c.370C>G	ENSP00000357122.9:p.Arg124 Gly
1	158908881	A	C	HET	0.000154	PYHIN1	nonsynonymous SNV	ENST00000368140:c.423A>C	ENSP00000357122.9:p.Lys141 Asn
8	31001099	T	A	HOM	NA	WRN	nonsynonymous SNV	ENST00000298139:c.3343T>A	ENSP00000298139.5:p.Cys111 5Ser
12	114387907	T	A	HOM	0.001922	RBM19	nonsynonymous SNV	ENST00000261741:c.1053A>T	ENSP00000261741.5:p.Lys351 Asn
19	7521294	G	A	HOM	NA	ARHGEF18		ENST00000359920:c.1617+5G>A	n/a
19	8175953	C	T	HET	0.001153	FBN3	nonsynonymous SNV	ENST00000270509:c.4199G>A	ENSP00000270509.2:p.Arg140 OGln
19	8188682	C	T	HET	0.001008	FBN3	nonsynonymous SNV	ENST00000270509:c.2942G>A	ENSP00000270509.2:p.Arg981 Gln
22	21044431	G	A	HOM	NA	POM121L4 P	nonsynonymous SNV	ENST00000412250:c.113G>A	n/a
22	22042011	G	A	HOM	0.000308	PPIL2	nonsynonymous SNV	ENST00000335025:c.977G>A	ENSP00000334553.8:p.Arg326 Gln

Table S6: Additional biallelic rare (ExAC MAF \leq 0.005) variants of unknown significance in *ARHGEF18* present in 4 individuals with unrelated phenotypes in the UCL exome cohort of 5695 individuals.

Individual	dbSNP	Genomic coordinates (GRCh37)	cDNA change (NM_001130955)	Protein consequence	Genotype	Homozygous individuals in gnomad dataset	Causative mutation identified	SIFT, Polyphen2 prediction
A	rs375852625	chr19:g.7505169G>A	c.343G>A	p.Gly115Arg	homozygous	0	no	D, PD
B	rs200483329	chr19:g.7516147C>T	c.1286C>T	p.Thr429Met	homozygous	0	yes	D, PD
C	rs28489511	chr19:g.7505332C>A	c.506C>A	p.Pro169Gln	heterozygous	13	no	T, B
C	rs74497723	chr19:g.7506936A>T	c.794A>T	p.Tyr265Phe	heterozygous	9	no	T, B
D	rs368588291	chr19:g.6516071G>A	c.1210G>A	p.Val404Leu	homozygous	0	yes	D, Poss D

D=Damaging, PD=Probably Damaging, T=Tolerated, B=Benign, Poss D=Possibly Damaging

Table S7: Clinical summary

Individual, family number	Age of onset, years, symptoms	Age at last review (length of review), years	Presenting VA logMAR (Snellen)	Latest VA logMAR (Snellen)	Latest refractive error, dioptres	Fundus features	Age at last electrophysiology, key findings	Colour vision	Visual fields	Other findings
Individual 1 GC18203	20 yrs reduced acuity, mild nyctalopia, blind spots	37 (8)	R 0.3 (20/40) L 0.18 (20/30)	R 0.6 (20/80) L 0.6 (20/80)	R 0/-0.50 x 100 L +1.00/-0.75 x 110	Irregular peripheral pigment, pale discs, cystoid macular edema, vitreous opacities, attenuated sheathed vessels, peripheral retinal exudate	30, subnormal PERG, rod specific ERG markedly subnormal, bright flash subnormal with unusual bifid b waves, cone specific delayed and subnormal; profound rod>cone dysfunction	Ishihara age 29 R 17/17 L 13/17	Octopus visual fields age 36 central 20-30 degrees retained on R , 30-50 degrees on L, age 37 24-2 central scotomas, fields now constricted to 15 degrees each eye	Nil else
Individual 2 GC3626	29, photopsia, slightly reduced acuity, mild nyctalopia	51 (22)	R 0.48 (20/60) L 0.3 (20/40)	R 1.8 (20/1250) L 1.5 (20/630)	R -1.00/-1.00 x 5 L +0.75/-1.00 x 90	Irregular pigmented lesions in periphery, pale discs, cystoid macular edema, peripheral telangiectasia with some retinal edema and vitreous cells, possible para-arteriolar sparing	29, no identifiable responses other than a minimal, delayed response to 30Hz flicker (PERG, EOG and ERG tested); severe photoreceptor dysfunction	Ishihara age 29 15/15 each eye	Goldmann visual fields age 29: ring scotoma at 30 degrees, binocular Esterman age 36: central 20 degrees only retained	L Fuch's heterochromic cyclitis
Individual 3 GC17880	30, photopsia, nyctalopia and field defects	38 (8)	R 0.18 (20/30) L 0.48 (20/60)	R 0.18 (20/30) L 0.8 (20/125)	R +2.25/-1.00 x5 L +2.00/-1.50 x 165	Irregular pigmented lesions in periphery, foveal/parafoveal cysts	30, PERG borderline on R, subnormal on L, undetectable rod ERG, abnormal cone ERG; severe rod>cone dysfunction	Ishihara age 33 R 21/23 L 3/23	Fields to confrontation age 36 years less than 30 degrees	Left band keratopathy Wolf-Parkinson White syndrome, 4 miscarriages

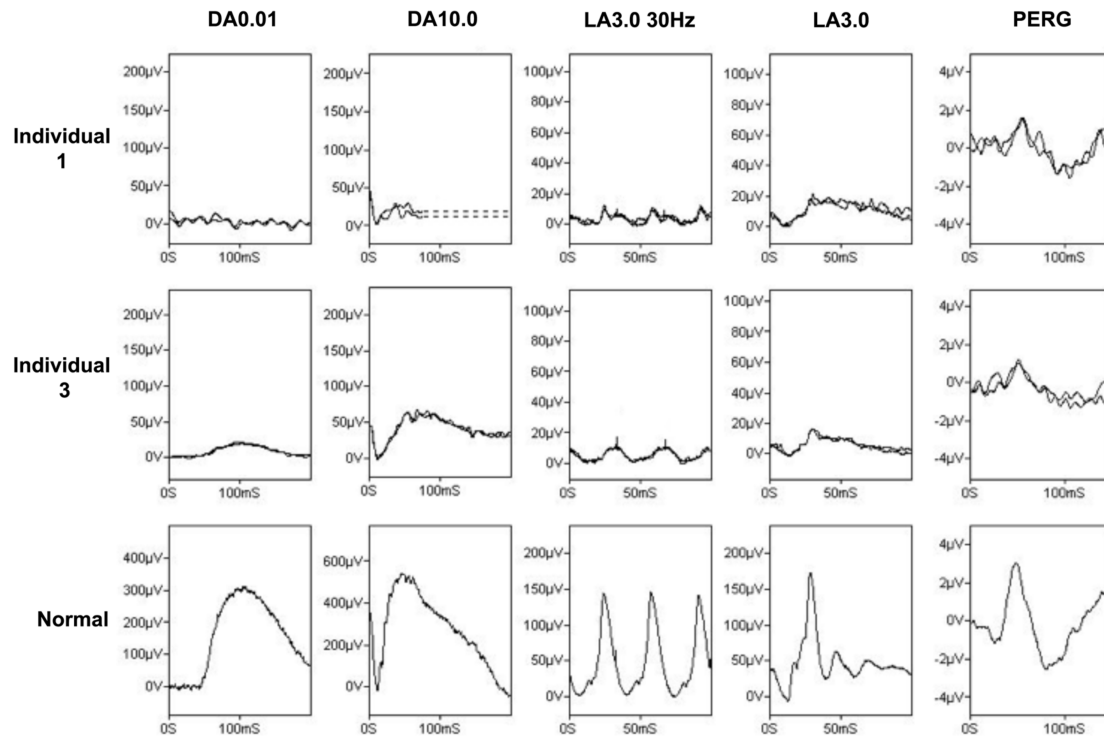


Figure S1: Full-field and pattern ERGs in individuals 1 and 3. DA: dark adapted; LA: light adapted. The numbers refer to flash strength (cd.s/m^2). The dim flash, rod-system specific ERG is severely reduced in individual 1; undetectable in individual 3. The bright flash DA 10 ERG is markedly subnormal in individual 1, and has a b-wave of lower amplitude than the a-wave in individual 3, perhaps suggesting the response to be arising in dark adapted cones in the absence of rod function. 30Hz flicker ERG is markedly reduced and delayed in individual 1; markedly reduced and of altered waveform in individual 3. Photopic single flash cone ERGs in both individuals are markedly subnormal and mildly delayed. PERG is mildly subnormal in both individuals. The findings are those of moderately severe (individual 1) or severe (individual 3) rod>cone dysfunction with macular involvement. Note difference in ERG amplitude scale in affected individuals compared with the representative normal traces.

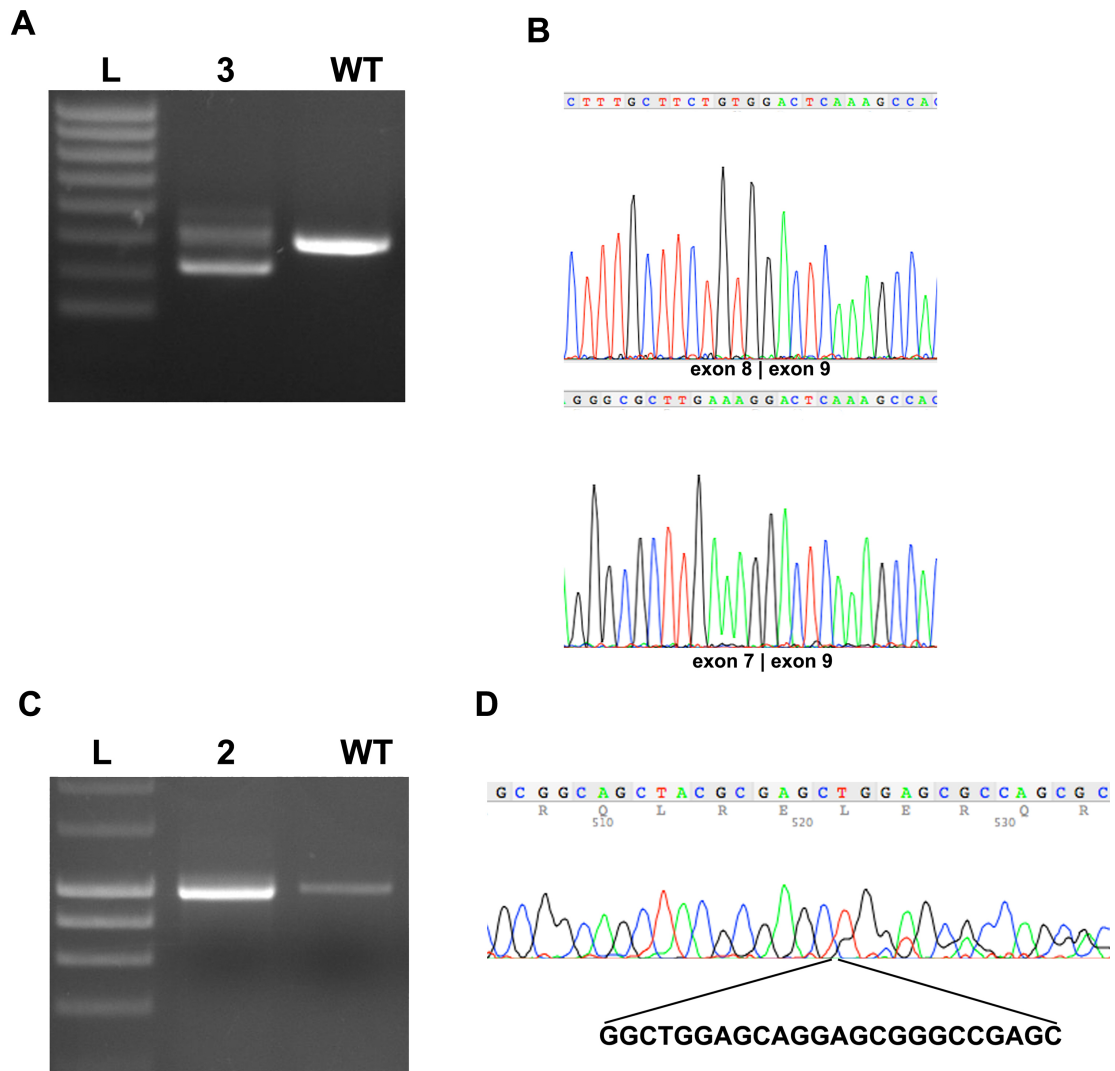


Figure S2: RT-PCR analysis of predicted splice-altering variants identified in *ARHGEF18*. **A:** Altered splicing due to c.1617+5G>A resulting in mixed transcripts comprising skipped exon 8 and wildtype (WT)(lane 3), L= ladder, WT= control RNA sample. **B:** Sanger sequencing of upper (top) and lower (bottom) bands from lane 3 showing normal splicing and skipping of exon 8 respectively. **C:** Mixed transcripts (lane 2) comprising c.2632G>T and c.2738_2761del alleles showing no splice alteration. **D:** Sanger sequencing of lane 2 band showing mixed alleles with heterozygous deletion of 24 nucleotides corresponding to c.2738_2761del.